$O(^1D_2\text{-}^3P_{2,1,0})$ 630.0, 636.4, and 639.2 nm Forbidden Emission Line Intensity Ratios Measured in the Terrestrial Nightglow†

B. D. Sharpee* and T. G. Slanger

Molecular Physics Laboratory, SRI International, Menlo Park, California 94025

Received: October 26, 2005; In Final Form: November 30, 2005

The intensity ratio of the neutral oxygen "red" emission lines $O(^1D_2-^3P_{2,1})$ 630.0 nm to 636.4 nm has been measured in terrestrial nightglow spectra obtained from astronomical instrumentation. The observed intensity ratio, I(630.0 nm)/I(636.4 nm) = 2.997 ± 0.016, is consistent with the value of 2.997 determined from the recent spontaneous emission coefficient calculations of Storey and Zeippen (2000), distinctly lower than the value of 3.10 calculated from those coefficients recommended by the National Institutes of Standards and Technology (NIST), and lower than the value of 3.1 measured by laboratory experiment (Kernahan and Pang, 1975). A weak emission line measured at 639.174 ± 0.003 nm has also been observed in these spectra and identified as the highly optically forbidden transition $O(^1D_2-^3P_0)$ 639.1773 nm of the same multiplet as the red lines. The observed intensity ratio, I(636.4 nm)/I(639.2 nm) = 1700 ± 700, is a factor of 2 lower than that predicted by most recent theoretical calculations.

1. Introduction

The $O(^1D)$ atom is a ubiquitous component of the atmosphere. During the day it is copiously generated in the stratosphere from ozone photodissociation in the Hartley band, whereas in the mesosphere and lower thermosphere, it is produced by O_2 photodissociation in the Schumann−Runge continuum. At night, $O(^1D)$ is produced by electron dissociative recombination of O_2^+ in the thermosphere,[1] whereas in aurorae it is produced by electron impact excitation of $O(^3P)$.[2] Being highly metastable with respect to radiation, its emission, via the optically forbidden transitions $O(^1D_2-^3P_{2,1})$ at 630.0 and 636.4 nm, can only be detected from high altitudes. Nevertheless, these extensively studied oxygen "red" emission lines are dominant components of thermospheric nightglow, dayglow, and aurora.

In actuality there are three emission lines associated with the $O(^1D-^3P)$ multiplet. Normally, the "red" designation refers to the two principal lines at 630.0 and 636.4 nm, of which the former is observed to be some 3 times as intense as the latter. However, this intensity ratio, which can only be single-valued because both lines arise from the same fine-structure level, has not been measured precisely by observation in the field or laboratory. Meanwhile, the much weaker third red line, $O(^1D_2-^3P_0)$ 639.2 nm, which proceeds by a much slower electric quadrupole (E2) transition than the magnetic dipole (M1)-dominated 630.0 and 636.4 nm red lines, has never before been observed.

Recently, several new ab initio calculations for the spontaneous emission coefficients governing these transitions have been carried out.[3−5] These newer calculation are mostly in agreement with one another, but differ from earlier, widely utilized values, such as those listed in Table 1. The apparent stability of the more recent calculations is important for the following reason. Differing choices of earlier-calculated coefficients have been cited as a source of conflicts between determinations of the rate coefficient for collisional quenching of ionospheric $O(^1D)$ by $O(^3P)$ inferred from observation and modeling of the 630.0 nm nightglow intensity.[1,6−8] This rate coefficient is important for determining the yield of $O(^1D)$ following electron dissociative recombination of O_2^+, a reaction important to the energetics of the thermosphere. Rate coefficients inferred from nightglow studies are generally much lower than those determined from ab initio calculations of O_2 potential curves,[9] scattering calculations involving experimentally observed O_2 decay products,[10] or by recent direct laboratory measurement.[11]

In light of the ongoing $O(^3P)$ on $O(^1D)$ quenching problem, the newer spontaneous emission coefficient calculations, and the importance of $O(^1D)$ as a prime atmospheric observable in the airglow, we have used our access to astronomical sky spectra[12,13] to make high precision determinations of the intensity ratios among the three oxygen red lines. The observed intensities of each line relative to one another should equal the corresponding ratios of sums of their M1 and E2 spontaneous emission coefficient components. Thus, we attempt to bring into line the results of field observations and calculations. The verification of $O(^1D_2-^3P_0)$ 639.2 nm in these spectra is also detailed.

2. Observations and Reductions

Spectra of the terrestrial nightglow were obtained from cooperative astronomers using the Echellette Spectrograph and Imager (ESI) on the Keck II telescope, W. M. Keck Observatory, Mauna Kea, HI, and were used previously in our investigation of the $N(^2D^o-^4S^o)$ 520 nm doublet intensity ratio.[13] The spectra used here consist of the absolute intensity calibrated spectra from the March, July, and October data sets of Sharpee et al.[13] (see their Table 2 for an observing log), with seven additional spectra from the March data set epoch not utilized previously. Spectra possess an instrumental spectral resolution ($\lambda/\Delta\lambda$) of 3200−5400, or about 0.12−0.20 nm at 636.4 nm. A portion of a typical spectrum near the red lines is shown in Figure 1.

In each spectrum the 630.0 and 636.4 nm emission line intensities were measured by fitting simultaneously their line

† Part of the special issue "David M. Golden Festschrift".

* Corresponding author: brian.sharpee@sri.com.

10.1021/jp056163x CCC: $33.50
Published on Web 01/24/2006

TABLE 1: Spontaneous Emission Coefficients *A* for O(^{1}D−^{3}P) Transitions, Associated Intensity Ratios, and Radiative Lifetimes *τ*(^{1}D)

reference	*A*(630.0 nm)[a] E2	*A*(630.0 nm)[a] M1	*A*(636.4 nm)[a] E2	*A*(636.4 nm)[a] M1	*A*(639.2 nm)[a] E2	*I*(630.0 nm)/*I*(636.4 nm)	*I*(636.4 nm)/*I*(639.2 nm)	τ(^{1}D) (s)
theoretical								
Garstang[19]	2.4(−5)	6.9(−3)	3.2(−6)	2.2(−3)	1.1(−6)	3.1	2000	110
Froese Fischer and Saha[20 b]	3.327(−5)	7.023(−3)	5.370(−6)	2.278(−3)	1.197(−6)	3.090	1908	107.1
Baluja and Zeippen[21 c]	1.917(−5)	5.608(−3)	3.065(−6)	1.815(−3)	8.922(−7)	3.095	2038	134.3
NIST[22]	2.11(−5)	5.63(−3)	3.39(−6)	1.82(−3)	8.60(−7)	3.10	2120	134
Galavís et al.[3]	2.218(−5)	6.513(−3)	3.754(−6)	2.107(−3)	6.388(−7)	3.096	3304	115.7
Storey and Zeippen[4]	2.218(−5)	6.424(−3)	3.754(−6)	2.147(−3)	6.388(−7)	2.997	3367	116.3
Froese Fischer and Taichev[5]	2.448(−5)	6.478(−3)	4.424(−6)	2.097(−3)	6.181(−7)	3.094	3400	116.2
experimental								
Kernahan and Pang[23]	5.15 ± 1.25(−3)		1.66 ± 0.42(−3)			3.1 ± 0.3		147
this paper						2.997 ± 0.016	1700 ± 700	

[a] In units of s^{-1}. Number in parentheses is the power of 10 by which the coefficient should be multiplied. [b] Results from “correlation calculation” ($m \geq 90$). [c] Authors’ “preferred values” with relativistic M1 (M1r) and theoretical energy correction (TEC).

TABLE 2: Most Likely Values *I*(630.0 nm)/*I*(636.4 nm) (ESI)

data set	order 9	order 10	all	num
March	2.98 ± 0.04	3.09 ± 0.04	3.03 ± 0.03	44
July	2.97 ± 0.04	2.96 ± 0.04	2.96 ± 0.03	36
October	2.98 ± 0.04	2.99 ± 0.04	2.99 ± 0.03	42
all	2.97 ± 0.02	3.02 ± 0.02	2.997 ± 0.016	122

profiles, those of nearby strong OH Meinel (9−3) band nightglow lines, a polynomial representing the continuum (scattered sunlight and scattered light within the spectrograph), and a solar spectrum[14] representing the level of Fraunhofer absorption in the scattered sunlight component of that continuum. The fit was repeated in both spectral orders (9 and 10), imaged simultaneously by the spectrograph, in which the lines appeared, doubling the number of measurements and providing a check on the accuracy of the relative intensity calibration. *I*(630.0 nm)/*I*(636.4 nm) was determined for individual data sets and for the combined data using a maximum probability analysis,[13] with results presented in Figure 2 and Table 2.

To search for the O($^1D_2$−$^3P_0$) 639.2 nm emission line, the 20 continuum-subtracted and Fraunhofer-corrected spectra of the highest available resolution ($\lambda/\Delta\lambda = 5400$) with the strongest and weakest 636.4 nm intensities were separately co-added together and compared. Spectra from both orders 9 and 10 were included in each co-addition. These selections group spectra taken early in the night, mostly within 3 h after sunset, and those taken toward the end of the night, mostly within 2 h before sunrise, roughly gauging the temporal behavior of the nightglow features they contain.

Both co-added spectra are presented in Figure 3. A feature near the predicted wavelength of the 639.2 nm line is present in the early night spectrum adjacent to the OH Meinel (9−3) $^QP_{21}$(3.5) satellite line at 639.344 nm, but absent in the late night spectrum, whereas the OH line intensity remains nearly constant. The intensity change of the putative 639.2 nm line mirrors those exhibited by features arising from known ionospheric processes such as electron radiative and dissociative recombination: O(^{5}P−^{5}S^o) 844.6 nm and the 630.0 nm red line itself. In contrast, features arising from chemical processes occurring in the mesopause and lower thermosphere, Na(^{2}P−^{2}S) 589.0 and 589.6 nm, the O_2 Atmospheric (0−1) band, O(^{1}S−^{1}D) 557.7 nm, and OH Meinel band system lines, show much smaller changes in intensity between the early and late night spectra. Therefore, the potential 639.2 nm line appears to have an ionospheric origin.

The co-added early night ESI spectrum, a similarly co-added spectrum obtained from the High Resolution Echelle Spectrophotometer (HIRES) on the Keck I telescope ($\lambda/\Delta\lambda = 34\,000-45\,000$, 0.014−0.019 nm at 636.4 nm), and a previously

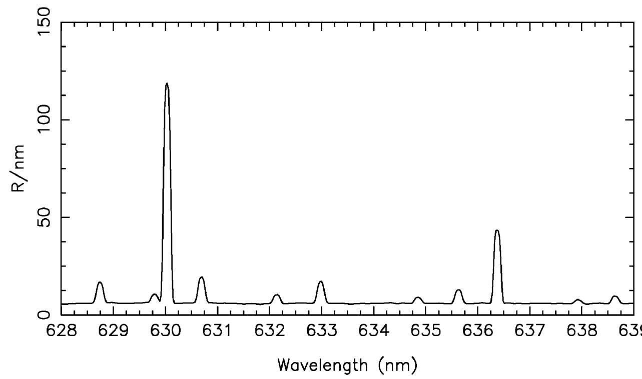

Figure 1. ESI nightglow spectrum (spectral order 10) from the October data set near the O($^1D_2$−$^3P_{2,1}$) 630.0 and 636.4 nm emission lines. Spectral resolution ($\lambda/\Delta\lambda$) is 4000, or 0.16 nm at 636.4 nm.

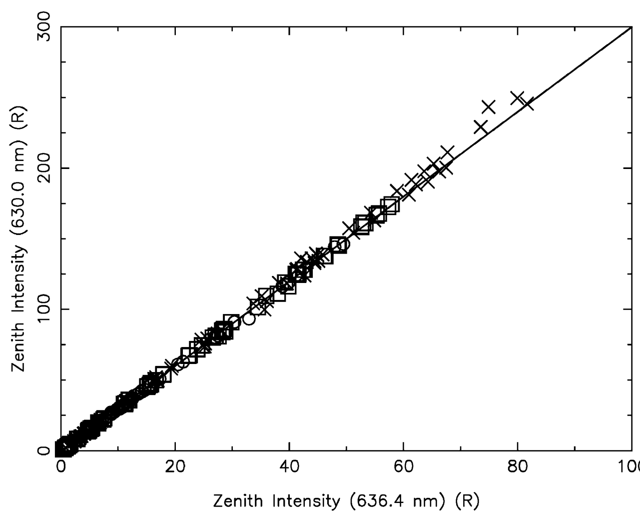

Figure 2. O($^1D_2$−$^3P_{2,1}$) 630.0 and 636.4 nm emission line intensities referred to zenith from the ESI March (crosses), July (circles), and October (squares) data sets, with most error bars internal to the symbols. The solid line is the most likely value of *I*(630.0 nm)/*I*(636.4 nm) for the combined ESI data (2.997).

published nightglow spectrum from the Ultraviolet Visual Echelle Spectrograph (UVES) on the VLT Kueyen Telescope at Paranal, Chile[15] ($\lambda/\Delta\lambda = 43\,000$, 0.015 nm at 636.4 nm) are shown in the vicinity of 639.2 nm in Figure 4, with the NIST O($^1D_2$−$^3P_0$) wavelength of 639.1774 nm indicated by a vertical dashed line. A feature is clearly present near this wavelength in all three spectra at roughly the same intensity relative to the OH Meinel (9−3) $^QP_{21}$(3.5) 639.344 nm line.

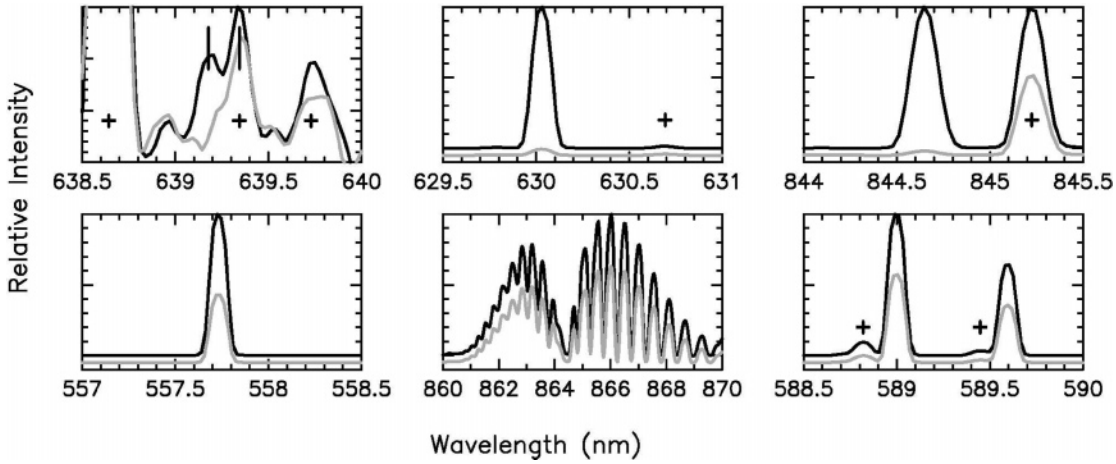

Figure 3. Co-added early night and late night (offset in gray) ESI spectra. Starting at the upper left and proceeding clockwise: $O(^1D_2-^3P_0)$ 639.2 nm, $O(^1D_2-^3P_2)$ 630.0 nm, $O(^3P-^3S^o)$ 844.6 nm triplet, $Na(^2P\text{-}^2S)$ 589.0 and 589.6 nm, the O_2 Atmospheric (0−1) band, and $O(^1S\text{-}^1D)$ 557.7 nm. Pluses mark positions of OH Meinel band system lines. Intensities are relative to the strongest peak intensity from the early night spectrum depicted in each panel. In the upper left panel, dashes indicate the NIST wavelength of $O(^1D_2-^3P_0)$ (639.1773 nm) and OH Meinel (9−3) $^QP_{21}(3.5)$ 639.344 nm.

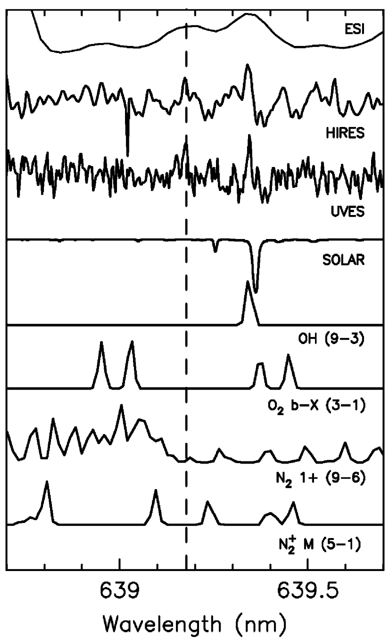

Figure 4. Co-added ESI (early night), HIRES, and UVES[15] spectra, a solar spectrum,[14] and DIATOM model spectra of the OH Meinel (9−3) (200 K),[16] O_2 Atmospheric (3−1) (200 K), N_2 First Positive (9−6) (1000 K),[17] and N_2^+ Meinel (5−1) (1000 K)[18] bands near 639.1773 nm (dashed line), presented at a spectral resolution ($\lambda/\Delta\lambda$) of 34 000 or 0.02 nm at 636.4 nm.

As also seen in Figure 4, the putative 639.2 nm feature does not match any strong line in model spectra of other nearby nightglow or auroral systems that were created with the DIATOM simulation code (http://www-mpl.sri.com/software/DIATOM/DIATOM.html). Furthermore, the strongest lines of these systems do not appear in any co-added or constituent spectrum. The feature is also not affected by Fraunhofer absorption. We therefore conclude that this feature is indeed $O(^1D_2-^3P_0)$ 639.2 nm, and present final measured wavelengths and I(636.4 nm)/I(639.2 nm) ratios in Table 3.

3. Discussion

As seen in Table 2, the I(630.0 nm)/I(636.4 nm) values determined from five of the six individual ESI data subsets are more consistent with the Storey and Zeippen[4] predicted value of 2.997, than with the consensus theory and experimentally determined value of ∼3.1. The higher March order 10 subset value, not replicated in order 9, results partially from a peculiarity in the automated data reduction process unique to this data set and order. Figure 2 shows that ratios determined from individual spectra cluster around the combined data set value of 2.997 over a wide range of line intensities, with high-intensity outliers belonging to the March order 10 data subset. The ratio measured from the UVES spectrum, 3.00 ± 0.06, also agrees well with the bulk of the ESI results.

TABLE 3: 639.2 nm Data Summary

instrument	I(636.4 nm)/ I(639.2 nm)	wavelength (nm)
ESI	3000 ± 2000	639.19 ± 0.03
UVES	1500 ± 800	639.174 ± 0.003
HIRES	1500 ± 1400	639.174 ± 0.007
adopted	1700 ± 700	639.174 ± 0.003

A possible explanation for a lower ratio is unaccounted-for absorption of the 630.0 nm emission in the nearby O_2 Atmospheric (2−0) band. Although a slight trend toward a lower ratio is seen in spectra with weaker 630.0 nm emission, the difference is not statistically significant when compared to the full range ratio value, nor do the spectra with the strongest 630.0 nm spectra yield a value approaching 3.1. Some inapplicability in using lower resolution (5 nm) tabulated spectrophotometric standard star spectra for intensity calibration in the vicinity of the O_2 absorption may also be to blame. Nevertheless, the UVES spectra, calibrated using master instrumental response curves independent of individual standard star observations, agrees well with the ESI values. Thus, because both red emission lines arise from the same fine structure level, it is difficult to envision another atmospheric process that would affect one line preferentially. This suggests that the observed intensity ratio purely reflects the atomic physics of the red line transitions. The agreement of the observed ratio with Storey and Zeippen does not alone definitively argue for the acceptance of their coefficients as standard. However, the fact that the observations do agree with their uniquely lower ratio, and the apparent consensus among the three most recent calculations of the $O(^1D)$ radiative lifetime, as seen in Table 1, suggests that an acceptable value for that lifetime, of 116 s, has been determined. This should be used for subsequent aeronomic studies.

Because the radiative lifetime is so long, emission from O(^{1}D) can only be seen at high altitudes, where the atmospheric density is low enough that radiation can effectively compete with quenching. In some previous studies combining the observed intensity of 630.0 nm nightglow emission with models of ionospheric chemistry, energetics, and transport,[1,7] the models used resulted in the best fit to observations when it was assumed that quenching of O(^{1}D) by O(^{3}P) was of little consequence. Recent laboratory experiment indicates that this is not the case,[11] and that O(^{3}P) is an important quencher of O(^{1}D) over a broad altitude range. In those previous nightglow studies, differences in assumed spontaneous emission coefficients for the red line transitions have been invoked to explain this discrepancy. Yet, the effect of quenching is much more pronounced than any remaining uncertainty in the radiative lifetime. Thus, the combination of the experimental confirmation of the theoretical red line intensity ratio with a demonstration that O(^{3}P) is an effective quencher of O(^{1}D) leads to the conclusion that further work is needed in understanding thermospheric O(^{1}D) sources and sinks.

The adopted wavelength of the 639.2 nm line and its intensity ratio with respect to the 636.4 nm line, reported in Table 3, were taken as the weighted average of the ESI, HIRES, and UVES spectra measurements of those values. The larger errors and intensity ratio measured in the ESI spectrum results from the lower resolution of the instrument, smearing out the line profile at a level comparable to the noise in the spectrum, and from lingering Fraunhofer absorption that together confuse the actual continuum level. Although the evidence from Figures 3 and 4 clearly suggests that a line is present in the ESI spectrum at the O($^1D_2-^3P_0$) 639.2 nm line's predicted wavelength, it is suspected that the true *I*(636.4 nm)/*I*(639.2 nm) ratio is closer to the HIRES and UVES values, coming from spectra that have line profiles and local continua levels near 639.2 nm that are easier to discern. The observed intensity ratio is a factor of 2 lower than that predicted by recent theory, including Storey and Zeippen. Older calculations have a larger 639.2 nm coefficient value and consequently a lower predicted intensity ratio with respect to 636.4 nm that agrees better with the observed ratio. This suggests that a larger 639.2 nm emission coefficient is needed.

4. Conclusions

The intensity ratio of the oxygen red lines O($^1D_2-^3P_{2,1}$) 630.0 nm to 636.4 nm, measured repeatedly in astronomical nightglow spectra, is found to be 2.997, consistent with the value predicted by Storey and Zeippen spontaneous emission coefficients, validating the necessity of the relativistic corrections made to those coefficients. These observations, along with the concordance of recent theoretical determinations of the O(^{1}D) radiative lifetime, suggest that a value of 116 s for that lifetime is appropriate for future aeronomic studies. A feature corresponding to O($^1D_2-^3P_0$) 639.2 nm has been observed in these spectra and identified as such due to its wavelength agreement with theory, the similarity of its temporal intensity characteristics to those of other known ionospheric nightglow lines, and the lack of sensible alternate IDs from other nightglow and auroral systems. The measured 636.4 nm to 639.2 nm intensity ratio disagrees by a factor of 2 with those predicted by the most recent theoretical calculations.

Acknowledgment. We gratefully acknowledge the astronomers who made their observations available to us. This paper is based on observations made at the W. M. Keck Observatory, which is operated jointly by the California Institute of Technology and the University of California. This work was supported by NSF grant ATM-0221700 and NSF CEDAR program grant ATM-0123136.

References and Notes

(1) Semeter, J.; Mendillo, M.; Baumgardner, J.; Holt, J.; Hunton, D.; Eccles, V. *J. Geophys. Res.* **1996**, *101*, 19683−19699.

(2) Solomon, S.; Hays, P.; Abreu, V. *J. Geophys. Res.* **1988**, *93*, 9867−9882.

(3) Galavís, M.; Mendoza, C.; Zeippen, C. *Astron. Astrophys. Supp.* **1997**, *123*, 159−171.

(4) Storey, P.; Zeippen, C. *Month. Not. Royal. Astron. Soc.* **2000**, *312*, 813−816.

(5) Froese Fischer, C.; Tachiev, G. *At. Data Nucl. Data Tables* **2004**, *87*, 1−184.

(6) Abreu, V.; Yee, J.; Solomon, S. *Planet. Space Sci.* **1986**, *34*, 1143−1145.

(7) Link, R.; Cogger, L. *J. Geophys. Res.* **1988**, *93*, 9883−9892.

(8) Sobral, J.; Takahashi, H.; Abdu, M.; Muralikrishna, P.; Sahai, Y.; Zamlutti, C. *Planet. Space Sci.* **1992**, *40*, 607−619.

(9) Yee, J.-H.; Guberman, S.; Dalgarno, A. *Planet. Space Sci.* **1990**, *38*, 647−652.

(10) Sun, Y.; A D. *J. Chem. Phys.* **1992**, *96*, 5017−5019.

(11) Closser, K.; Pejakoviæ, D.; Kalogerakis, K. *Eos Trans. AGU, Fall Meet, Suppl.* **2005**, *86*, SA11A0215.

(12) Sharpee, B.; Slanger, T.; Huestis, D.; Cosby, P. *Astrophys. J.* **2004**, *606*, 605−610.

(13) Sharpee, B.; Slanger, T.; Cosby, P.; Huestis, D. *Geophys. Res. Lett.* **2005**, *32*, L12106.

(14) Delbouille, L.; Roland, G.; Neven, L. *Atlas Photometrique DU Spectre Solarie de λ3000 a λ10000*; University Liege: Liege, 1973.

(15) Hanuschik, R. *Astron. Astrophys.* **2003**, *407*, 1157−1164.

(16) Coxon, J.; Foster, S. *Can. J. Phys.* **1982**, *60*, 41−48.

(17) Ferguson, D.; Narahari Rao, K.; Martin, P.; Guelachvili, G. *J. Mol. Spectrosc.* **1992**, *153*, 599−609.

(18) Huber, K.; Herzberg, G. *Constants of Diatomic Molecules*; Van Nostrand Reinhold Co.: New York, 1979.

(19) Garstang, R. *Month. Not. Royal. Astron. Soc.* **1951**, *111*, 115−124.

(20) Froese Fischer, C.; Saha, H. *Phys. R. A* **1983**, *28*, 3169.

(21) Baluja, K.; Zeippen, C. *J. Phys. B* **1988**, *21*, 1455−1471.

(22) Wiese, W., Fuhr, J., Deters, T., Eds. *Atomic Transition Probabilities of Carbon, Nitrogen, and Oxygen: a Critical Data Compilation*; American Chemical Society: Washington, DC, 1996.

(23) Kernahan, J.; Pang, P. H.-L. *Can. J. Phys.* **1975**, *53*, 455−458.